

SPS Vertical Aperture Studies

F. Roncarolo, G. Arduini

Abstract

We present the results of a series of measurements carried out in order to study the SPS physical aperture in the vertical plane. A vertical kick was applied to the circulating beam while introducing a closed orbit bump at the location of the SPS high energy beam dump absorber (TIDVG) that was suspected of limiting the aperture asymmetrically. Beam intensity and transverse profile measurements, performed before and after the kick, were combined to estimate the aperture.

Geneva, Switzerland

December 21, 2006

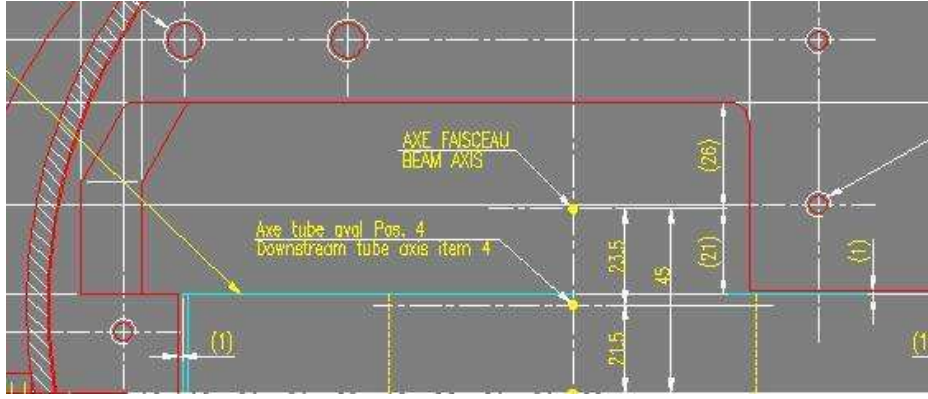


Figure 1: Cross section of the SPS high energy beam dump absorber TIDVG.

1 Introduction

Before the installation in the SPS machine, 5 Titanium foils were stretched over the internal beam dump TIDVG in order to prevent the release of graphite dust [1]. A drawing of the TIDVG cross section is shown in Figure 1

During the shut down period 2003-2004 a deformation of the foils was observed and the accelerator vertical aperture was suspected to be reduced at that element. For this reason, a series of measurements was performed during the 2004 run, with the following aims:

1. to verify that the internal beam dump limited the aperture;
2. to study means to recover part of the vertical SPS aperture by deforming locally the beam orbit (the aperture of the beam dump is asymmetric).

The measurement method consisted of the following steps:

- a fast transverse kick was applied over one machine turn; before and after the kick, the beam intensity and the vertical transverse profile were measured;
- a closed orbit bump was introduced around the location of the internal dump, in order to displace the closed orbit far from the obstacle (the deformed foil); then the kick, the beam intensity and the beam profile measurements were repeated;
- the above step was repeated with different amplitudes of the closed orbit bump.

2 Kick method model

At a location s around the ring, the normalized phase space $(Y_n(s), Y'_n(s))$ coordinates in the vertical plane are defined by

$$Y_n(s) = \frac{y(s)}{\sqrt{\beta(s)}} \quad (1)$$

$$Y'_n(s) = \frac{\alpha(s)}{\sqrt{\beta(s)}}y(s) + \sqrt{\beta(s)}y'(s) \quad (2)$$

In this coordinate system, for stable motion, equi-density contours of the transverse distribution are circles. Initially, the particles are distributed around the reference position $Y_n = 0$. If a transverse kick with amplitude $K(s_0)$ is applied at turn 0 and

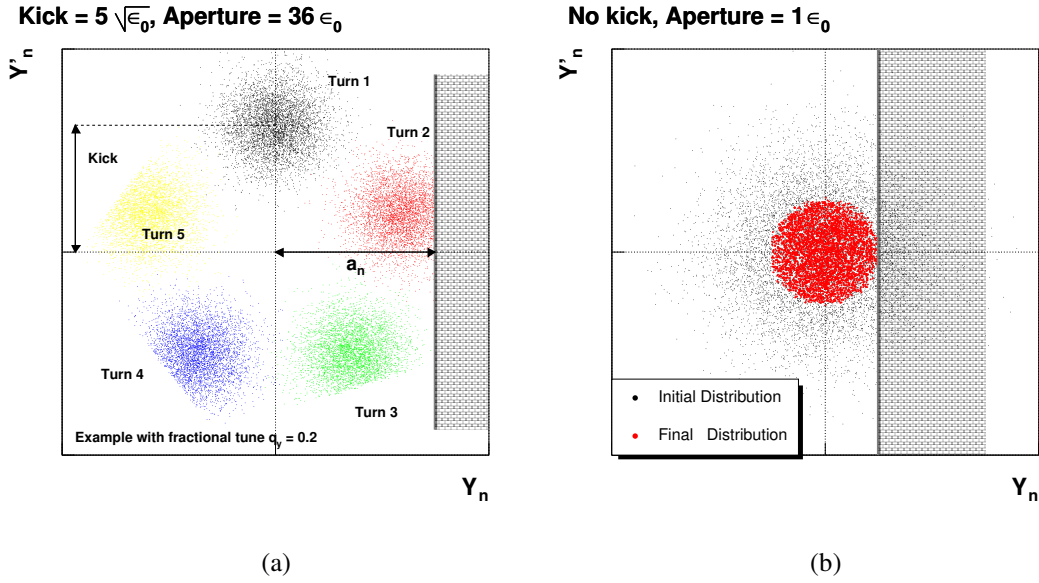


Figure 2: Tracking of the particle portrait in normalized phase space: (a) case with a kick much larger than the initial beam size and (b) case with no kick.

at the location s_0 , the particles start orbiting on a circumference with radius equal to $K_n = K(s_0)\sqrt{\beta_y(s_0)}$. The portion of circumference covered for each turn is determined by the fractional part of the tune, as shown in Figure 2(a).

If the kick amplitude is sufficient to displace the particles towards an obstacle that limits the aperture, a portion of the beam is lost during the turns following the kick.

If a_n is the physical aperture limit in normalized phase space, then the accelerator aperture can be expressed in terms of its acceptance:

$$A = a_n^2[m] = \frac{y_{obstacle}^2}{\beta_y(s_{obstacle})}[m] \quad (3)$$

where $y_{obstacle}$ is the physical half aperture at the obstacle (assumed to be symmetric, defining the physical aperture of the machine, and $\beta(s_{obstacle})$ the betatron function amplitude at the obstacle location.

2.1 Estimate of the aperture by monitoring the beam intensity

The measurement of the beam intensity before and after the kick allows a first estimate of the aperture limit to be calculated.

Approximation $K_n \gg \sqrt{\epsilon_0}$

Given the initial RMS beam emittance ϵ_0 , in the case of a Gaussian beam and of a kick amplitude such that $K_n \gg \sqrt{\epsilon_0}$ (see the example of Figure 2(a)), the percentage of lost particles can be easily determined.

For instance, if the initial Gaussian parameters are the mean μ_0 (corresponding to the kick amplitude) and the standard deviation σ_0 corresponding to the RMS beam size, a 16%

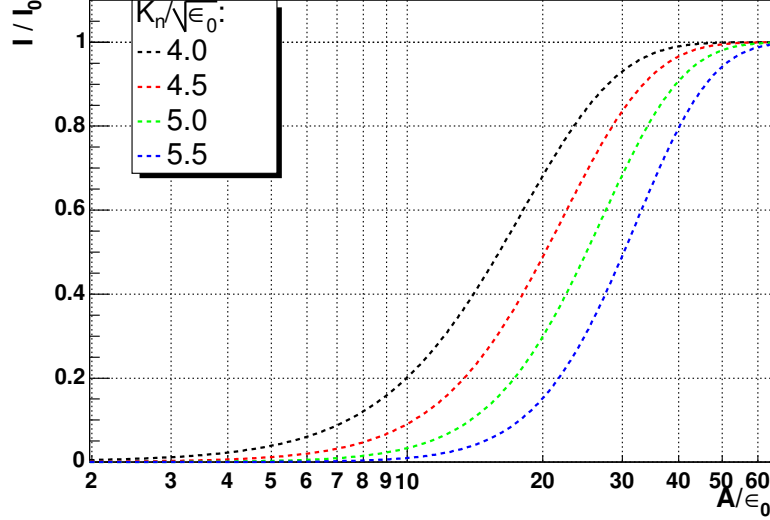


Figure 3: Expected relative beam intensity after the kick as function of the aperture, for large kicks $K_n \gg \sqrt{\epsilon_0}$.

decrease of the intensity indicates that all particles at $Y_n \geq (\mu_0 + \sigma_0)$ are lost. Therefore, knowing the kick amplitude K_n , the aperture limit can be expressed as

$$a_n = K_n + Y_n^{cut} \quad (4)$$

The relative beam intensity as expected from the scraping of the Gaussian profile is shown in Figure 3 for different aperture values.

This approximation is only correct if the amplitude of oscillations remains constant during the beam intensity measurement. Such a condition, that could not be verified during the measurements presented here, can be violated if a transverse feedback system is acting on the beam.

More general case

This covers also the case in which $K_n \approx \sqrt{\epsilon_0}$ and accounts for the occurrence of filamentation.

In this case the above approximation does not apply as it can be understood from the following simple example. Assuming to have a small aperture in units of initial RMS beam emittance, losses can be observed even without applying any kick¹. In such a condition the beam losses can be calculated by means of the phase space bi-variant Gaussian distribution integral: all particles orbiting in normalized phase space at a radius larger than the aperture are lost, as shown in Figure 2(b).

If the initial particle density distribution is a bi-variant Gaussian in normalized phase space, its expression in polar coordinates is

$$\rho_0(r, \theta) = \frac{1}{2\pi\epsilon_0} \exp\left[-\frac{r^2}{2\pi}\right], \quad \text{with } r = \sqrt{Y_n^2 + Y_n'^2} \quad (5)$$

¹This is the case of another aperture measurement method that consists in increasing on purpose the emittance until when the beam halo is scraped by the aperture

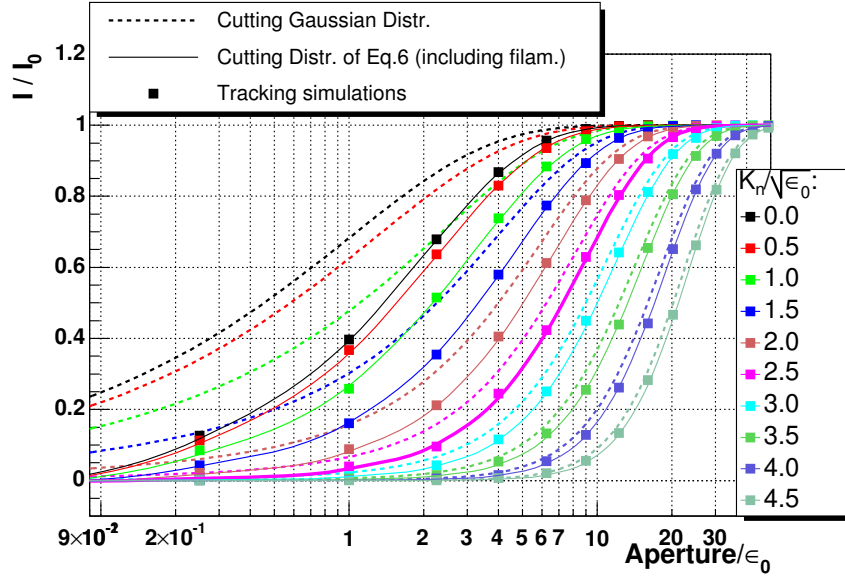


Figure 4: Expected relative beam intensity after the kick as function of the aperture, for different kick amplitudes as calculated by the analytical model based on Eq. (6) (solid lines) and by tracking simulations (square dots). The analytical prediction calculated according to the Gaussian profile (dashed lines) scraping is indicated too.

After the kick and the occurrence of filamentation, the particle density distribution is represented by [2]:

$$\rho_{fil}(r, \theta) = \frac{1}{2\pi\epsilon_0} \exp\left[-\frac{r^2}{2\pi} H\right] \cdot I_0\left[\frac{r^2}{2\epsilon} \sqrt{H^2 - 1}\right] \quad (6)$$

$$\text{with } H = 1 + \frac{K_n^2}{2\epsilon_0}$$

and $I_0[x]$ = Modified Bessel function of order 0

In the presence of an aperture limitation $A = a_n^2$ as defined in Eq. (3), after a large number of turns and with non fractional tune, all particles at $r > a_n$ are lost and the fraction of remaining particles can be calculated as:

$$\frac{I}{I_0} = \frac{\int_{r=0}^{a_n} \int_{\theta=0}^{2\pi} \rho_{fil}(r, \theta) r dr d\theta}{\int_{r=0}^{\infty} \int_{\theta=0}^{2\pi} \rho_{fil}(r, \theta) r dr d\theta} \quad (7)$$

In order to cross-check such a formulation, we developed a set of tracking simulations of the particle distribution in phase space in order to estimate the aperture limit by measuring the beam losses. The results are shown in Figure 4 as relative remaining beam intensity versus aperture limit, for different kick amplitudes. The results of the tracking simulations are indicated by the square dots, while the values based on Eq. (6) and Eq. (7) are plotted as solid lines. The agreement between the two methods is excellent.

In the same figure, the dashed lines represent the analytical prediction using the large-kick approximation described in the previous paragraph. It is thus verified that for small kicks, such an approximation underestimates the beam losses (i.e. predicts a smaller aperture for a given beam loss).

2.2 Estimate of the aperture by monitoring the transverse distribution

If the transverse distribution is measured after the kick and after the losses induced by the aperture limit, the beam profile is expected to exhibit a sharp cut of the distribution tails. In general, a transverse profile measurement takes several turns to be completed and filamentation occurs. As discussed in the previous paragraph, the distribution after filamentation can be predicted analytically (see Eq. (6)). The effect of filamentation on the distribution in phase space is shown in Figure 5 which is the output of a tracking simulation. Turn 0 is immediately after the kick while at turn 1500 the distribution has reached the new equilibrium after filamentation. Figure 6 shows the projection on the normalized vertical coordinate of the final distribution as predicted by both the tracking and the analytical formula of Eq. (6). Two cases with different kick and aperture values are illustrated. In the tracking an obstacle was introduced at a given amplitude from the center of the initial distribution. The cut of the final distribution tails leads to the estimate of the aperture.

Therefore the available aperture can be measured:

- by comparing the beam intensity before and after the kick if the kick amplitude is known as a function of the initial beam size;
- by measuring the transverse profile after the kick.

In both cases, the evolution of the beam position with time needs to be measured.

3 Measurements

The measurements were performed on the SPS fixed target cycle of supercycle 950. The vertical kick was applied on the injection plateau at 14 GeV , 0.5 s after the beginning of the cycle. Before presenting the measurement results, the calibration of the vertical kick must be considered. As discussed in the introduction above, the knowledge of the kick amplitude is in fact necessary for the accurate determination of the physical aperture.

3.1 Kicker Calibration

The calibration of the vertical kicker MKQV was studied through a dedicated experiment carried out on a different date from the aperture studies presented in this note. The vertical beam trajectory at all the available SPS Beam Position Monitors (BPM) was recorded for about 1000 turns after applying a kick. The experiment was repeated for two values of the kicker voltage, $V_1 = 8\text{ kV}$ and $V_2 = 10\text{ kV}$. Figure 7 shows the signal of 4 BPMs for 2 turns before the kick and 7 turns after. The dots indicate the measured values, while the solid lines represent a sinusoidal fit to the data. The sinusoid frequency is fixed by the fractional part of the vertical betatron tune, while the amplitude, obtained from the fit, assesses the oscillation amplitude and therefore the kick strength.

In normalized phase space, the oscillation amplitude should ideally be identical at all the BPMs. The distribution of the normalized oscillation amplitude, as measured by all the BPMs at the two kicker voltage settings, is shown in Figure 8. The calibration result is summarized in Table 3 in terms of mean kick amplitude μ and considering the error on the mean $\sigma_\mu = \sigma/\sqrt{N}$ as the measurement error. In addition, the table indicates the kick

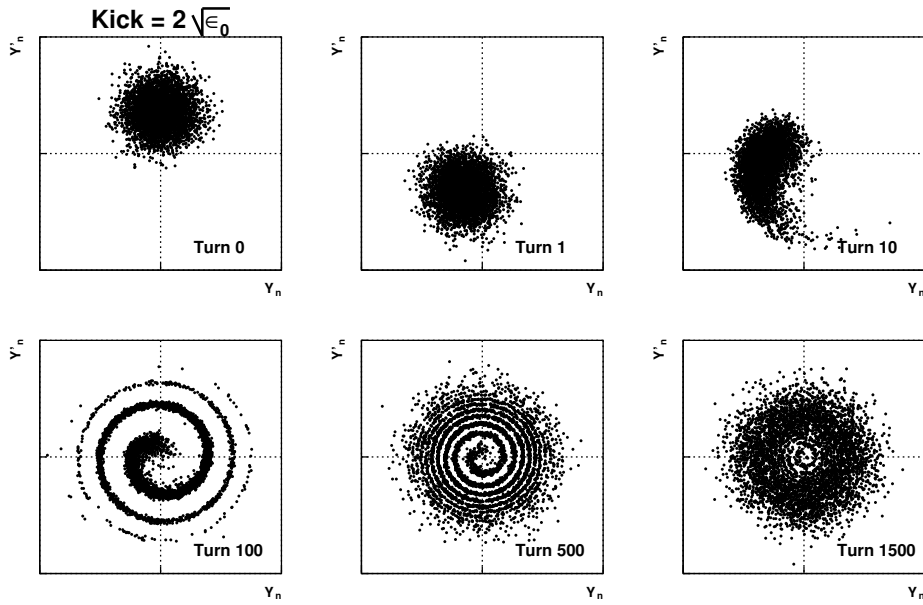


Figure 5: Phase space portraits after the kick, accounting for filamentation. If ϵ_y is the single particle emittance, the used amplitude detuning factor is $dQ_y/d\epsilon_y = 50$ [3].

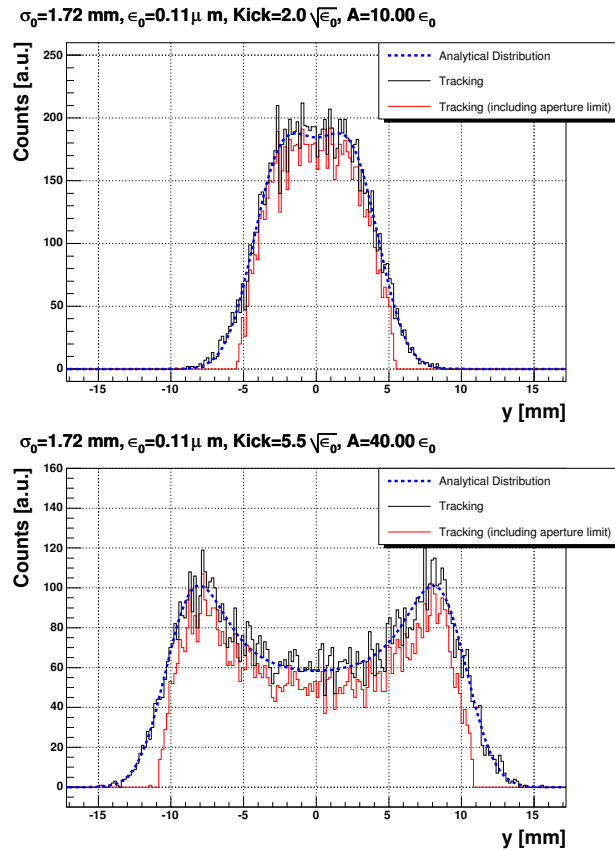


Figure 6: Analytical prediction and tracking simulation of the transverse beam profile (at the location of one of the SPS wire scanner monitors (BWS51995), where $\beta_y = 27.8 m$) after the kick and filamentation, for two different cases of kick and aperture values. The simulations provide the beam profile after 1500 turns and include (red line) the aperture model.

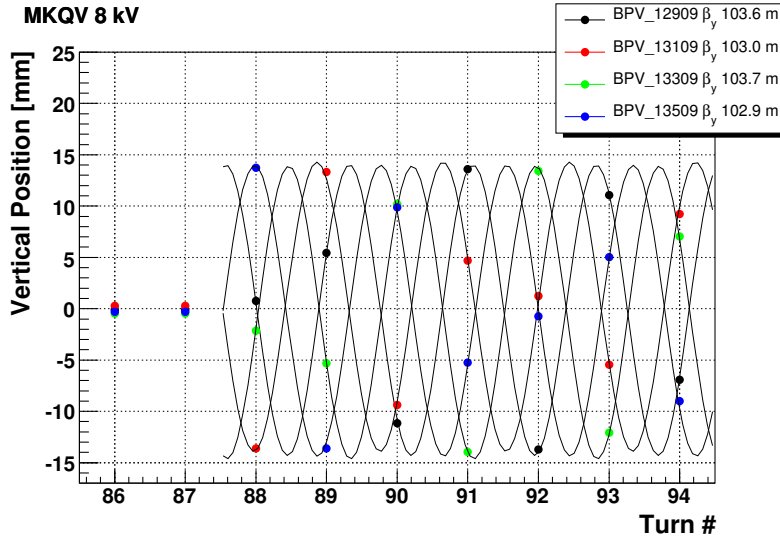


Figure 7: Example of the beam trajectory oscillation as measured by 4 vertical BPMs before and after the kick. Dots are measurements whereas lines are the sinusoidal fits from which the oscillation amplitude is inferred.

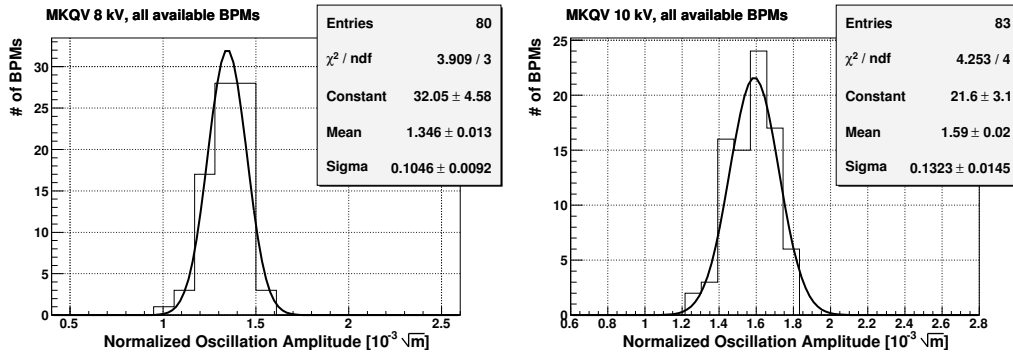


Figure 8: Distribution of the normalized oscillation amplitude as measured by all the available BPMs at the two kicker voltages applied during the calibration.

Kicker Voltage	N BPMs	Kick Amplitude		
		$\mu[10^{-3}\sqrt{m}]$	$\sigma_{\mu}[10^{-3}\sqrt{m}]$	$\sigma_{\mu}/\mu[\%]$
8 kV	80	1.346	0.013	1.0
10 kV	83	1.590	0.020	1.2
5 kV	/	0.98	/	/

Table 1: Kicker calibration results: measured kick amplitude at 8 and 10 kV and extrapolated value at 5 kV.

normalized amplitude one should consider for the aperture measurements, for which the kicker voltage was set to 5 kV , after a linear extrapolation from the two measured values. The linear extrapolation provides a kick larger than zero when no voltage is applied to the kicker, indicating a non-linearity of the kicker response to its power supply, as expected from the powering hardware [4]. In absence of a calibration over the entire dynamic range, we adopted the linear extrapolation as the best available approximation.

3.2 Remarks on the closed orbit bump

The amplitude of the closed orbit bump was programmed and measured at the vertical BPM BPD11906. The actual amplitude at the internal dump can be computed knowing the corrector strengths used to introduce the bump and the accelerator optics. The calculations obtained using MAD give a beam displacement of 0.94 mm at the dump, when the closed orbit bump is programmed to have an amplitude of 1 mm at BPD11906. This 6% difference has been used to compute the amplitude of the bumps at the dump that will be quoted in the next sections.

In addition, being the bump location close to the SPS injection region, the correction of beam orbit oscillations after injection had to be performed for each change of the bump amplitude.

3.3 Beam intensity measurements

The beam intensity was measured by means of one of the SPS DC current transformers (DCCT) and sampled every 10 ms (corresponding to approximately 430 turns). The result of the measurements is shown in Figure 9, where the beam intensity is plotted as a function of time for each cycle. Dots stand for the mean values over different cycles and the error bars indicate the error on the mean. As explained in the legend, different colors correspond to various amplitudes of the closed orbit bump at the beam dump location.

The occurrence of the kick at $t = 0.5\text{ s}$ is clearly correlated to beam losses in the first $10 - 20\text{ ms}$ after the kick. The decrease of the beam intensity at $t = 1.3\text{ s}$ is correlated with the start of acceleration (at $t=1.26\text{ s}$) and is not relevant for our results.

The values of the relative beam losses after the kick are shown in Figure 10 as function of the bump amplitude. When no bump is applied the losses reach almost 25%. Displacing the closed orbit at a larger distance from the graphite absorber, located below the beam aperture (i.e. positive values of the bump, see Figure 1), causes a decrease of the losses, that reach a minimum of about 12% when the bump amplitude is set between 3.76 and 5.64 mm . Continuing to increase the bump amplitude again induces a loss increase, since the beam starts to hit the opposite side of the beam dump aperture.

3.4 Transverse Profile Measurements

Two wire scanner monitors (BWS51731 and BWS51995) equipped with Carbon wires of $30\text{ }\mu\text{m}$ diameter, installed at two locations 90 m apart, were used to measure the vertical profile distribution. Table 2 lists the basic characteristics of the two wire scanners. Four profile examples (one for each instrument, before and after the kick) are shown in Figure 11. As expected, the effect of the kick is the enlargement of the beam profile, since the wire scanner monitors sample the projection of the particle distribution on the vertical plane, similar to the one simulated in Figure 6. The non-Gaussian tails visible in the profiles before the kick are less evident in the profiles after the kick. However, the

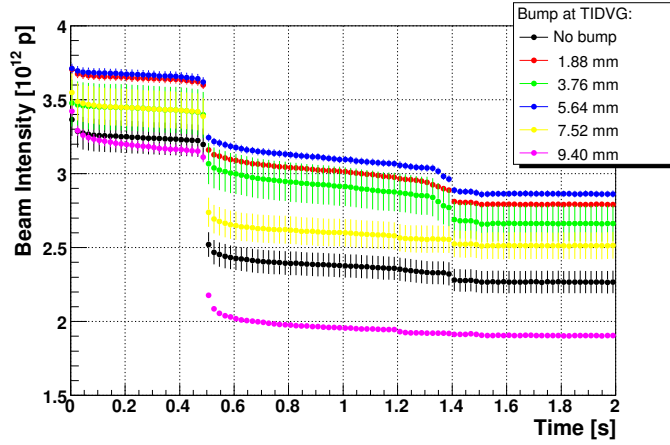


Figure 9: Beam intensity as measured for different closed orbit bump amplitudes, when the beam is kicked with a 5 kV kick at $t = 0.5\text{ s}$

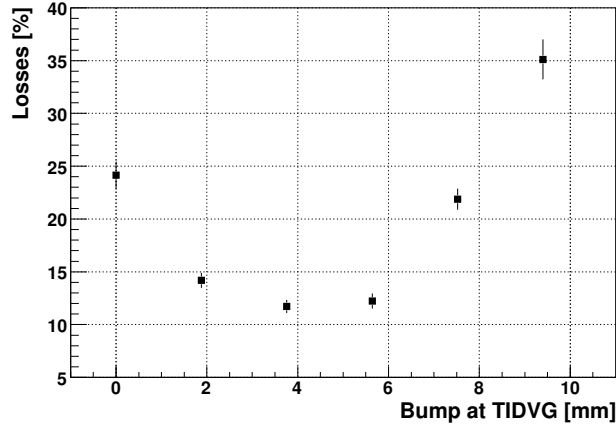


Figure 10: Relative beam losses after the kick for the different bump amplitudes.

Monitor	Mechanism	Wire Speed [m/s]	β_y [m]
BWS51731	Linear	1	98
BWS51995	Rotational	6	28

Table 2: Main features of the two wire scanner monitors used for the vertical profile measurements

distribution cut caused by an aperture limit, as foreseen by the model, is not observable. This can be well explained by the fact that the measurement is taken 500 ms after the kick and during this period the oscillation amplitude could have changed under the effect of the transverse feedback.

Figure 12 shows how the physical aperture is determined by analyzing the beam profiles after the kick. The transverse coordinates at which the profile amplitude drops to the baseline level are considered as the distribution cut induced by the aperture limitation. It must be noted that if the beam oscillation amplitude induced by the kick was damped before

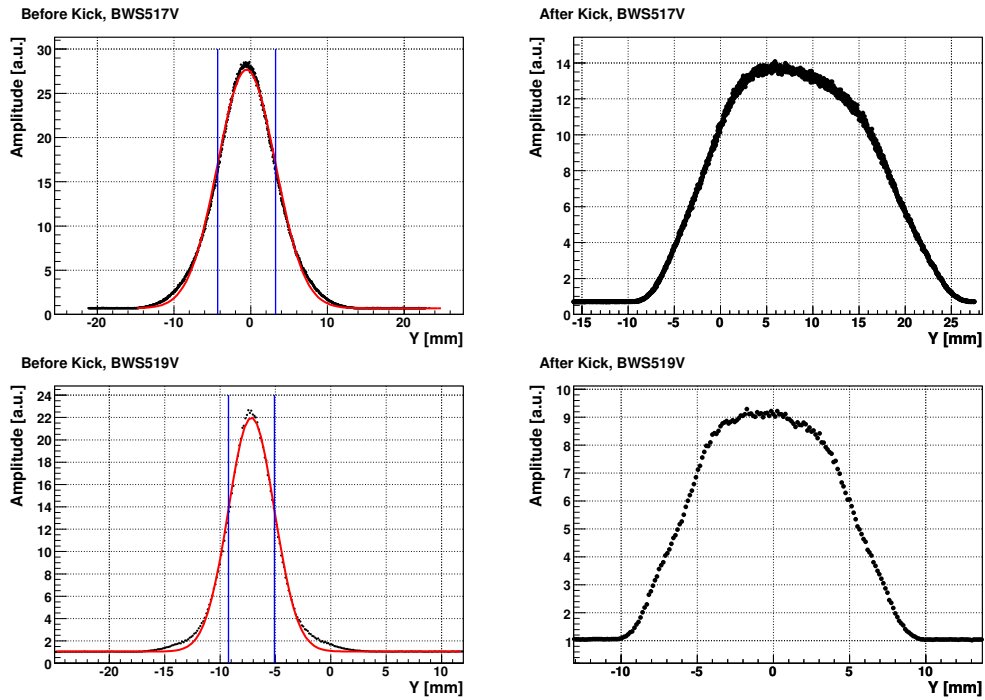


Figure 11: Examples of transverse profile measurements before and after the kick, with two SPS Wire Scanners. The blue lines on the left plots delimit the $\pm 1\sigma$ extent.

the profile measurement, the aperture determined with this method would be smaller than the real one (i.e. it would be a pessimistic estimate). Unfortunately, measurements of the beam oscillation amplitude after the kick are not available.

The measured physical aperture as function of the amplitude of the closed orbit bump at the internal dump location is shown in Figure 13. The three different colors indicate:

black: results of the beam profile measurements with BWS519V;

red: results of the beam profile measurements with BWS51995 when including in the analysis a systematic error in the wire position determination that was corrected in 2003. These results are meant to serve as a comparison with similar measurements carried out with the same monitor in the previous years, when the error was not yet known;

blue: results of the beam profile measurements with BWS51731.

As a first conclusion, the plot verifies the accuracy of the systematic error correction on the wire position determination for BWS519V. In fact, such an error was only related to rotational devices (i.e. BWS517V was not concerned) and the agreement between the two monitors is improved after the error correction. The larger discrepancy between the two instruments is about 2.5 % for bump amplitudes of 3.76 and 5.64 mm.

The aperture estimate shown in Figure 13 confirms the information provided by the beam intensity measurements (see Figure 10): displacing the orbit far from the internal dump increases the aperture value, until a position is reached when the opposite side of beam pipe becomes the aperture limitation.

The maximum available aperture is obtained for the bump amplitudes equal to 3.76 and 5.64 mm, in perfect agreement with the beam intensity measurements (see Figure 10).

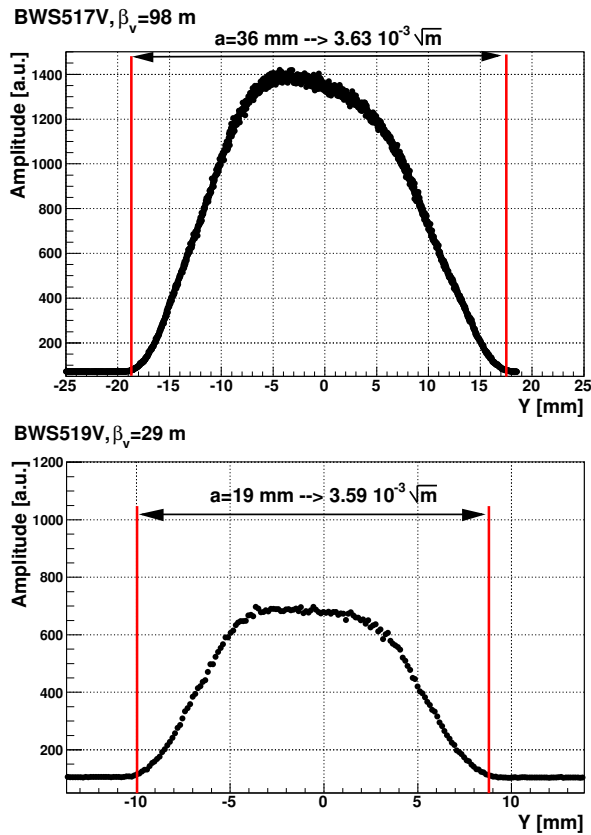


Figure 12: Estimate of the normalized vertical aperture from the two SPS wire scanners.

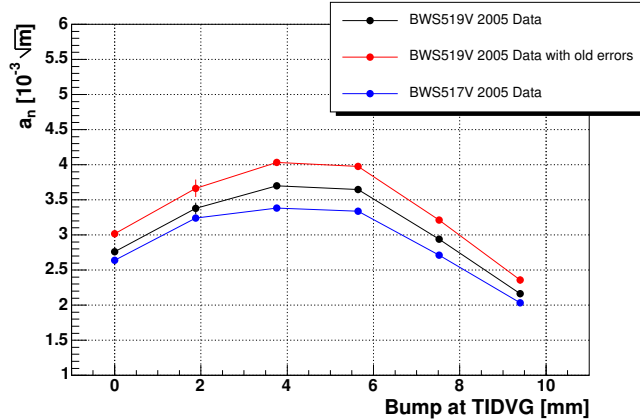


Figure 13: Aperture values as measured by the two wire scanners for the different bump amplitudes.

3.5 Summary of the measurement results

The aperture limit can be estimated from the beam intensity measurements with a closed orbit bump of 3.76 mm at the dump location. Considering:

- the measured relative losses of about 12 %,
- the kick amplitude $K_n = 0.980 \cdot 10^{-3} \sqrt{m}$, as determined from the kicker calibration,
- the initial RMS emittance (not normalized) as measured at the WS $\epsilon_0 = 0.16 \mu m$,

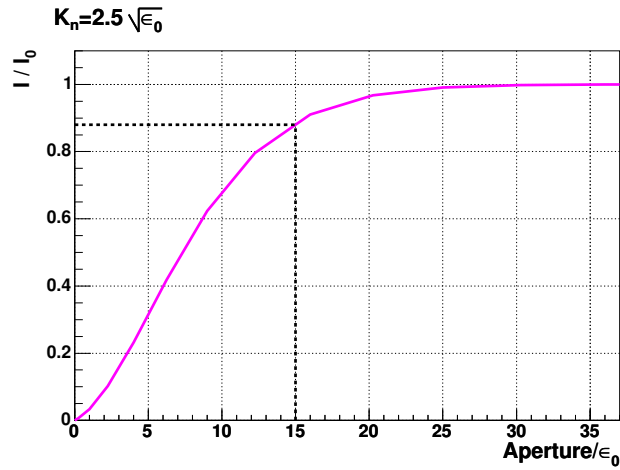


Figure 14: Estimate of the acceptance from the measured beam intensity and kick amplitude.

one can infer the aperture value from the tracking simulation plots of Figure 4 by taking the curve corresponding to a kick amplitude of about $2.5 \sqrt{\epsilon_0}$, as shown in Figure 14. Therefore, the corresponding acceptance results:

$$A_1 \approx 15 \epsilon_0 = 2.4 \mu m$$

The aperture estimate obtained from the transverse profile monitors gives

$$a_n \approx 1.80 \cdot 10^{-3} \sqrt{m} \implies A_2 \approx 3.24 \mu m$$

The two results A_1 and A_2 are not compatible. The disagreement could be due to an erroneous estimate of the kick amplitude, which may arise from:

1. an error in the kicker calibration described in Section 3.1;
2. the onset of a fast transverse instability leading to an increase of the oscillation amplitude, above the one initially provided by the kicker;
3. the presence of important non Gaussian tails.

Both A_1 and A_2 values are significantly smaller than the expected physical aperture limit, which is about $4.5 \mu m$.

Conclusions

The studies presented in this note confirm the hypothesis that the internal beam dump TIDVG constituted a limitation of the SPS vertical aperture, due to a deformation of the Titanium foils that were stretched over it. Beam intensity and transverse profile measurements indicate that the aperture increases when a closed orbit bump is applied at the dump location. The Titanium foils have been removed during the SPS shut-down 2004-2006. When the bump amplitude was set between 3.7 and 5.6 mm, the kick method allowed us to estimate the maximum aperture available. The results of beam intensity measurements, tracking simulations and transverse profile measurements exhibit a discrepancy of about

30 % in terms of physical aperture. The estimated acceptance results between 2.40 and 3.24 μm . Such a value is significantly smaller than the expected physical aperture of about 4.5 μm .

It is recommended repeating the measurements in the next SPS run, at first to verify the effectiveness of the Titanium foils removal from the internal dump and then to check the new aperture limit. The measurement accuracy can be improved in the following way:

- the beam trajectory after the kick should be recorded. Thus, the kick amplitude would be determined independently from the kicker calibration and taking into account any variation of the oscillation amplitude;
- the synchronization of the kicker magnet and of the beam position monitors with respect to the beam passage should be adjusted in order to kick and measure the same portion of the longitudinal distribution;
- the SPS Ionization Profile Monitor could be used in addition to the Wire Scanners. Even though the absolute calibration of the IPM is still in a development stage, it represents a non intercepting method to measure the transverse beam size and accurately determine its variation every 20 *ms*. This would give meaningful information that can be correlated with the beam intensity evolution;
- the measurements with the wire scanners should be performed before the kick and just after it, in order to minimize the dependence of the results on the evolution of the beam oscillation amplitude (damping due to the transverse feedback or growth due to instabilities);
- the measurements should be performed at low beam intensity in order to avoid the use of the transverse feedback.

Acknowledgments

The authors would like to acknowledge all the members of the OP group who helped in the measurements. Many thanks to S.Redaeli and R.Tomas for the fruitful discussions.

References

- [1] O. Aberle, ATB Issues, Presentation at the CERN PS-SPS Days 2006, <http://indico.cern.ch/contributionDisplay.py?contribId=5&sessionId=1&confId=183>
- [2] G. Arduini, P. Raimondi, Transverse emittance blow-up due to injection errors, CERN SL-Note-99-022-SLI
- [3] R.Tomas, *Amplitude detuning values from SPS measurements at 14 GeV in 2003 (private communication)*.
- [4] G. Vossenberg , *Private communication*